Int. J. Appl. Math. Comput. Sci., 2026, Vol. 36, No. 3, 493–503
DOI: 10.61822/amcs-2026-0032

ADAPTIVE ITERATIVE LEARNING CONTROL OF MULTI–AGENT SYSTEMS UNDER ITERATIVE BATCH RANDOM MISSING FAULTS BASED ON NEURAL NETWORKS

XINGJIAN FU [a,*], YUHAN LI [a]

[a] School of Automation
Beijing Information Science and Technology University
No. 12, Xiaoying East Road, Haidian District, Beijing, China
e-mail: {fxj,2023020456}@bistu.edu.cn

For multi-agent systems with missing iteration batches and randomly varying lengths, a data-driven adaptive iterative learning control strategy based on neural networks is proposed. Considering the situation where the iteration batches of the system vary randomly with the number of iterations, first, an iterative batch missing fault model that follows a random probability distribution is designed. Secondly, based on the radial basis function neural network method, a novel data-driven adaptive iterative learning consistency control algorithm is proposed. The stability analysis of the system is strictly performed using the Lyapunov function, and the sufficient conditions for consistency of multi-agent systems are derived through relevant mathematical derivations. This enables multi-agent systems to achieve state consistency even when there are missing faults in the iterative batches. Finally, the feasibility of the algorithm is verified through numerical simulations in a multi-agent system.

Keywords: multi-agent system, consistency, iterative learning control, data-driven, iterative batch random variation.

1. Introduction

Multi-agent systems are composed of multiple autonomous agents, which are capable of interacting with each other (Zhang and Li, 2024). With the rapid development of computer communication technology, researchers have extended the concept of a single-agent to a multi-agent system, focusing on the communication and collaboration between agents to enhance work efficiency and performance in addressing complex real-world problems (Wang *et al*., 2016). In the past few decades, the problem of collaborative control in multi-agent systems has received significant attention in various fields, including robotic control systems, unmanned aerial vehicle systems, and autonomous driving systems (Postoyan *et al*., 2015; Dong *et al*., 2016; Gao *et al*., 2018; Xie *et al*., 2018; Li and Gao, 2018). The core challenge of collaborative control lies in achieving consensus, that is, designing appropriate control strategies to ensure that the output states of multiple agents ultimately achieve synchronization in control.

With the growing demands in production as well as the increasing complexity and diversity of industrial environments, significant challenges have emerged for multi-agent systems. To address them, a considerable body of research has been devoted to studying multi-agent systems under various complex and dynamic conditions. In the work of Xiao *et al*. (2023), the impact of multiple uncertainties on nonlinear stochastic multi-agent systems is considered, and a novel continuous fully distributed consensus control protocol is designed. In the paper by Zhang *et al.* (2024b), an impulsive consensus protocol is employed to investigate the consensus problem of a Lipschitz multi-agent system under deception attacks and random disturbances. Rehan *et al*. (2018) employ relative state feedback to address the consensus problem of a multi-agent system under amplitude-bounded disturbances and communication topology switching. A convex cooperative control scheme based on graph theory for a multiagent system of differential mobile robots in a leader–follower formation is proposed by López-Estrada *et al*. (2024). The convergence of the controller is guaranteed by a non-quadratic Lyapunov function, and the

*Corresponding author

distributed consensus of the followers is achieved.

Iterative learning control is an important branch of learning control and represents a novel strategy. It controls the system through an initial control law and then compares the error between the output and the desired trajectory to adjust the control signal, thereby improving the system's tracking performance (Fu *et al*., 2017). Lv *et al*. (2024) propose a novel robust distributed localization estimation algorithm based on iterative learning, which investigates the real-time localization problem of a dynamic multi-agent system with measurement and communication noise under a directed graph. In the work of Zhang *et al.* (2024a), a control input compensation scheme based on iterative learning control is proposed for a nonlinear multi-agent system with quantization and arbitrary initial states. Wu *et al*. (2023) design a distributed P-type iterative learning consensus control protocol based on network topology information and nearest-neighbor knowledge to address the consensus control problem of a nonlinear pulse distributed parameter multi-agent system with time-dependent dynamic behavior. In the work of Peng *et al*. (2024), the consensus learning control problem of a nonlinear multi-agent system under false data injection (FDI) attacks is studied, effectively reducing the impact of the latter. Jiaqi *et al*. (2018) consider the iterative learning consensus tracking problem of a nonlinear multi-agent system under data transmission loss. All this highlights why the use of iterative learning control algorithms to study multi-agent system consensus is the primary motivation of this paper.

However, the exploration of multi-agent systems with unknown dynamic models has been limited. It is well known that, for increasingly complex industrial processes and highly precise equipment, obtaining the dynamic model of the controlled system using traditional system identification methods faces significant challenges. Fortunately, a model-free adaptive control strategy framework has been proposed by some scholars. It designs the controller using only the input-output data of the controlled system (Hou *et al*., 2017). Bu *et al*. (2019) propose a distributed model-free adaptive iterative learning control (MFAILC) method for a class of unknown nonlinear multi-agent systems to achieve consensus tracking. In the work of Liu and Hou (2023), a novel model-free adaptive iterative learning control scheme for the constrained control problem of unknown heterogeneous nonlinear multi-agent systems with bounded measurable and unmeasurable disturbances is introduced. Jinli *et al*. (2023) propose a model-free adaptive iterative learning control (MFAILC) algorithm, which investigates the finite-time convergence tracking control problem of a multi-agent system under periodic denial-of-service (DoS) attacks. Therefore, model-free iterative learning control, which only considers the system's input-output data, is the other motivation of this paper.

In iterative learning control, the stochastic variation of the iterative batch itself refers to the randomness in the occurrence or sequence of the batches. This includes phenomena such as randomly varying iteration lengths (where the duration of each trial differs stochastically), random trial skipping, or the stochastic absence of certain batch processes, which means the index of the effective iteration is no longer deterministic but follows a certain random distribution. Such stochastic variations can affect the convergence and tracking performance of ILC; therefore, in practical applications, robust ILC, stochastic ILC, or adaptive methods are often required to ensure system stability and learning efficacy. The aforementioned studies all focus on iterative learning under the assumption of complete iteration batch lengths. When the duration of each iteration varies randomly, maintaining tracking performance becomes a key focus of research. Shen *et al*. (2016) introduce an iterative learning control (ILC) method for discrete-time affine nonlinear systems with random iteration length variations. In the work of Li *et al*. (2014), an ILC scheme using an iterative averaging operator is proposed, which investigates discrete-time linear systems where the trial period length may vary randomly during the iteration process. A few researchers have also considered the case of varying iteration batches in multi-agent systems. Liang *et al*. (2019) studied the distributed iterative learning control of a nonlinear discrete multi-agent system with randomly varying iteration lengths . It is evident that research on the possible occurrence of random iteration batch variations in multi-agent system iterative learning control is scarce, and only traditional iterative learning control methods have been considered.

Based on the above research, a model-free adaptive iterative learning control strategy is proposed in this paper, considering the random variation of iteration time lengths in multi-agent system iterative learning. Additionally, the pseudo-partial derivatives are estimated online using the RBF neural network. The main contributions of this paper are as follows:

1. A model-free iterative learning control method is used, where the control input relies solely on the system's input-output data for consensus control.

2. Considering the random variation of iteration batch lengths, a probabilistic mechanism is introduced, which ensures that the iteration time length of the multi-agent system differs in each iteration.

3. To address the instability caused by the random variation of iteration batches, an RBF neural network is used to estimate the pseudo-partial derivatives

online, enabling the system to achieve convergence more effectively and quickly.

This innovation ensures that the system can maintain good robustness in complex and dynamic real-world engineering applications, providing a new approach to addressing the consensus problem of a multi-agent system in complex dynamic environments. Finally, the effectiveness of the algorithm is validated through numerical simulations.

2. Preliminaries and problem formulation

2.1. Graph theory. In the study, graph theory is utilized to describe the network communication topology among agents in a multi-agent system. Each agent in the system is considered to be a node, and thus the set of all agents can be represented as a node set $V = \{1, 2, \cdots, N\}$. The set of edges between nodes is denoted by $\varepsilon = V \times V$. The communication between nodes can be described using the weighted adjacency matrix $A = (a_{ij}) \in R^{n\times n}$. The weights can represent the influence of the information.

The three parts above constitute $G = \{V, \varepsilon, A\}$, representing the communication topology of a multi-agent system. In the adjacency matrix $A = (a_{ij}) \in R^{N\times N}$, where i and j represent two different nodes. The set of neighboring nodes of the i-th node can be denoted using $N_i = \{j \in V : (i, j) \in \varepsilon, i \neq j\}$. If $a_{ij} = 0$ exists, it represents $(i, j) \notin \varepsilon$, indicating that there is no communication relationship between node i and node j. If the topology graph is undirected, both $(i, j) \in \varepsilon$ and $(j, i) \in \varepsilon$ exist. Otherwise, the topology graph is a directed one. In graph theory, the Laplacian matrix is important for analyzing the topology graph G and is defined as follows: $L = D - A$, where $D = diag(d_1, d_2, \cdots, d_n)$ is the in-degree matrix of the topological structure, and the in-degree of node i is defined as $d_i = \sum_{j=1}^{n} a_{ij}$. Leaders can be one or multiple individuals. Let the set of nodes representing the leaders be denoted by $\overline{V} = V \cup \{v_0\}$, and let S $= diag\{s_1, s_2, \cdots s_N\}$.

2.2. Iteration batch missing fault. In practical system operation, due to the uncertainty of the external environment, partial missing data in each agent's iteration batch may occur during a single learning iteration, meaning the iteration batch lengths may not be the same. The actual iteration batch length T_k is varied randomly with each iteration. $T_{\min}$ represents the minimum length of the iteration batch, and the length of each iteration batch varies randomly within the discrete interval $\{T_{\min}, \ldots T_{\max}\}$. For the control input update, the output information when $t = 0, 1, \cdots, T_{\min}$ is accessible during each iteration of the learning process. However, the output information can only be partially obtained when $t = T_{\min} + 1, \ldots, T_{\max}$. That is, there is a missing iteration batch length in the interval $\{T_k + 1, \ldots, T_{\max}\}$, and the system is unable to update the output information. Therefore, in the interval where iteration batch length is missing, correct output information cannot be obtained. Only the data prior to the missing iteration can be updated through iterative learning.

Traditional ILC relies on tracking errors throughout the entire iteration cycle to update control signals. When batch lengths vary randomly, shorter batches truncate the error signal, resulting in loss of high-frequency or terminal tracking information. Discarding this incomplete data directly reduces learning efficiency; using incomplete data for updates may introduce erroneous correction signals.

2.3. Problem description. The multi-agent system designed in this paper is modeled so that each agent is assumed to satisfy the following dynamic model:

$$\begin{aligned} y_{i,k}(t) = f_i[&y_{i,k}(t-1), \cdots y_{i,k}(t-n_y), \\ &u_{i,k}(t-1), \cdots u_{i,k}(t-n_u)]. \end{aligned} \tag{1}$$

In this formulation, k is defined as the number of iterations, $t \in [T_{\min}, T_{\max}]$, $u_{i,k}(t)$ and $y_{i,k}(t)$ are denoted as the input and output of agent i at the k-th iteration, $f_i(\cdot)$ is represented as an unknown nonlinear function, while n_u and n_y are considered to denote the unknown orders of $u_i(\cdot)$ and $y_i(\cdot)$. The desired trajectory of the given multi-agent system is denoted by $y_d(t)$. When the iteration time length is incomplete, the tracking error is represented as $e_{i,k}(t) = y_d(t) - y_{i,k}(t)$ within the time interval prior to T_k. After T_k, the trajectory satisfies $e_{i,k}(t) = 0$. Therefore, the tracking error can be expressed as

$$e^*_{i,k}(t) = \begin{cases} e_{i,k}(t), 0 \le t \le T_k, \\ 0, t > T_k. \end{cases} \tag{2}$$

The consensus error of the system is given as

$$\begin{aligned} \xi^*{}_{i,k}(t) = &\sum_{j\in N_i} a_{ij} \left(y^*{}_{j,k}(t) - y^*{}_{i,k}(t)\right) \\ &+ s_i \left(y_d(t) - y^*{}_{i,k}(t)\right), \end{aligned} \tag{3}$$

where a_{ij} is defined as the weight between agents, If the agent is connected to the leader, then s_i>0; otherwise, $s_i = 0$. Also, $y^*_{k,i}(t)$ is defined as the output under randomly varying iteration batches.

3. Design of iterative learning control with neural networks

In general research, dynamic linearization techniques are typically employed to transform nonlinear systems into linear time-varying systems. Here, the compact form

dynamic linearization (CFDL) method is employed. It is assumed that, for each agent i, at every time step t of each k-th iteration, there exists a pseudo-partial derivative $\phi_{i,k}(t)$ (PPD) such that the system satisfies

$$\Delta y_{i,k}(t+1) = \phi_{i,k}(t)\Delta u_{i,k}(t), \tag{4}$$

where $\triangle\, y_{i,k}(t+1) = y_{i,k}(t+1) - y_{i,k}(t)$ and $\triangle\, u_{i,k}(t) = u_{i,k}(t) - u_{i,k}(t-1)$. This assumption requires the system to be generalized Lipschitz.

Since the pseudo-partial derivative $\phi_{i,k}(t)$ is unknown and may vary with each iteration, an RBF neural network (RBFNN) is used to estimate this value online. The output of the RBFNN is considered to be

$$\hat{\phi}_{i,k}(t) = \omega_{i,k}^{T}(t)h[z_{i,k}(t)], \tag{5}$$

where $\hat{\phi}_{i,k}(t)$ is the estimated value of the pseudo-partial derivative $\phi_{i,k}(t)$, $\omega_{i,k}(t)$ is the weight vector, $h(\cdot)$ is the output vector of the hidden layer, with $h[z_{i,k}(t)] = \exp(-\frac{\|z-\alpha\|^2}{2r^2})$, α is the center vector, and r is the width. Additionally, $z_{i,k}(t) = [y_{i,k}(t), y_{i,k}(t-1), \cdots y_{i,k}(t-n_y+1), u_{i,k}(t-1), u_{i,k}(t-2), \cdots u_{i,k}(t-n_u+1)]$, which represents the input layer in the RBFNN.

In this paper, the gradient descent method is employed to update the neural network weights, with the objective of minimizing the estimation error:

$$\begin{aligned} &J(\omega_{i,k}(t)) \\ &= \frac{1}{2}\left(y_{i,k}(t+1) - y_{i,k}(t) - \hat{\phi}_{i,k}(t)\Delta u_{i,k}(t)\right)^2, \end{aligned} \tag{6}$$

where $\hat{\phi}_{i,k}(t)$ and $\triangle\, u_{i,k}(t)$ do not depend on the weights $\omega_{i,k}(t)$, and are considered constants when computing the gradient. The parameters are set to $\frac{\partial y_{i,k}(t)}{\partial \omega_{i,k}} = h[z_{i,k}(t)]\ \triangle\, u_{i,k}(t)$ and $\frac{\partial y_{i,k}(t+1)}{\partial \omega_{i,k}} \approx 0$.

Remark 1. Since the weights $W_{i,k}(t)$ have not yet been updated, $y_{i,k}(t+1)$ may be predicted based on the current weights, but its gradient is difficult to obtain accurately. In the dynamic evolution of the system, the primary reliance is on the information available at the current time step.

Therefore, the weight update rule is given by

$$\begin{aligned} &\omega_{i,k}(t+1) \\ &\quad = \omega_{i,k}(t) - \eta\frac{\partial J}{\partial \omega_{i,k}} \\ &\quad = \omega_{i,k}(t) - \eta\frac{\partial J}{\partial e}\cdot\frac{\partial e}{\partial \omega_{i,k}} \\ &\quad = \omega_{i,k}(t) - \eta\frac{\partial J}{\partial e}\cdot\frac{\partial}{\partial \omega_{i,k}}\left(y_{i,k}(t+1) - y_{i,k}(t)\right) \\ &\quad = \omega_{i,k}(t) - \eta\frac{\partial J}{\partial e}\cdot\left(\frac{\partial y_{i,k}(t+1)}{\partial \omega_{i,k}} - \frac{\partial y_{i,k}(t)}{\partial \omega_{i,k}}\right). \end{aligned} \tag{7}$$

Considering iterative learning, the knowledge transfer between weight update iterations is as follows:

$$\omega_{i,k+1}(0) = \omega_{i,k}(T_k), \tag{8}$$

where $\lambda > 0$ is the weight factor used to limit the variation of the control input.

The control objective function is represented by

$$J\left(u_{i,k}\left(t\right)\right) = \frac{1}{2}\left(\xi_{i,k}^{*}\left(t+1\right)\right)^2 + \frac{\lambda}{2}\left(\Delta u_{i,k}\left(t\right)\right)^2. \tag{9}$$

According to the dynamic linearization model, we have

$$\xi_{i,k}^{*}(t+1) \approx \xi_{i,k}^{*}(t) + \frac{\partial \xi_{i,k}^{*}(t+1)}{\partial u_{i,k}(t)}\Delta u_{i,k}(t). \tag{10}$$

Based on the consistency error (3), the following is derived:

$$\frac{\partial \xi_{i,k}^{*}(t+1)}{\partial u_{i,k}(t)} = -\left(\sum_{j\in N_i} a_{ij} + s_i\right)\hat{\phi}_{i,k}(t). \tag{11}$$

Remark 2. It is assumed here that the dependency of the control input on the output variations of neighboring agents is reflected through their respective PPDs. However, for simplicity, the influence of neighboring agents is primarily considered in terms of the agent's own control input, and it is assumed that the influence from neighbors remains unchanged over short periods.

Therefore, let

$$\hat{\xi}_{\mathrm{i,k}}(t+1) = \xi_{i,k}^{*}(t) - \left(\sum_{j\in N_i} a_{ij} + s_i\right)\hat{\phi}_{i,k}(t)\Delta u_{i,k}(t) \tag{12}$$

and

$$\begin{aligned} &J\left(u_{i,k}\left(t\right)\right) \\ &= \frac{1}{2}\left[\xi_{i,k}^{*}\left(t\right) - \left(\sum_{j\in N_i} \alpha_{ij} + s_i\right)\hat{\phi}_{i,k}\left(t\right)\Delta u_{i,k}\left(t\right)\right]^2 \\ &\quad + \frac{\lambda}{2}\left(\Delta u_{i,k}\left(t\right)\right)^2. \end{aligned} \tag{13}$$

The optimal solution can be obtained by deriving the extremum

$$\frac{\partial J}{\partial \Delta u} = 0. \tag{14}$$

Simplifying, the following is obtained:

$$\Delta u_{i,k}\left(t\right) = \frac{\rho\left(\sum_{j\in N_i} a_{ij} + s_i\right)\hat{\phi}_{i,k}\left(t\right)\xi_{i,k}^{*}\left(t\right)}{\lambda + \left(\sum_{j\in N_i} a_{ij} + s_i\right)^2\hat{\phi}_{i,k}^{2}\left(t\right)}. \tag{15}$$

Therefore, the iterative learning control law is given by

$$\begin{aligned} u_{i,k}(t) &= u_{i,k}(t-1) \\ &\quad + \frac{\rho\left(\sum_{j\in N_i} a_{ij} + s_i\right)\hat{\phi}_{i,k}(t)\xi_{i,k}^{*}(t)}{\lambda + \left(\sum_{j\in N_i} a_{ij} + s_i\right)^2\hat{\phi}_{i,k}^{2}(t)}. \end{aligned} \tag{16}$$

4. Convergence analysis

To analyze the convergence of the system, the following assumptions are given.

Assumption 1. The PPD is bounded and its sign remains unchanged:

$$0 < \phi_{\min} \leq |\phi_{i,k}(t)| \leq \phi_{\max}.$$

Assumption 2. There exists an ideal weight such that the approximation error is bounded:

$$\left|\phi_{i,k}(t) - \omega_i^{*T} h(z_{i,k}(t))\right| \leq \varepsilon_{\max}.$$

Assumption 3. The radial basis function is bounded:

$$0 < h_{\min} \leq |h(\cdot)| \leq h_{\max}.$$

Assumption 4. The weight update law is bounded:

$$|\omega_{i,k}(t)| \leq \omega_{\max}.$$

Lemma 1. (Weight convergence) *Under the weight update law, the weight error $\tilde{\omega}_{i,k}(t) = \omega_i^* - \omega_{i,k}(t)$ satisfies*

$$\begin{aligned}\|\tilde{\omega}_{i,k}(t+1)\|^2 &\leq \|\tilde{\omega}_{i,k}(t)\|^2 - 2\eta\delta_{i,k}(t)\Delta u_{i,k}(t)h^T\tilde{\omega}_{i,k}(t) \\ &\quad + \eta^2\delta_{i,k}^2(t)\|h\|^2\left(\Delta u_{i,k}(t)\right)^2,\end{aligned} \tag{17}$$

where

$$\delta_{i,k}(t) = y_{i,k}(t+1) - y_{i,k}(t) - \hat{\phi}_{i,k}(t) \triangle u_{i,k}(t).$$

Proof. From the weight update law (7), it follows that

$$\tilde{\omega}_{i,k}(t+1) = \tilde{\omega}_{i,k}(t) + \eta\delta_{i,k}(t)\Delta u_{i,k}(t)h^T\Delta u_{i,k}(t). \tag{18}$$

Taking the squared norm of both sides, it follows that

$$\begin{aligned}\|\tilde{\omega}_{i,k}(t+1)\|^2 &= \|\tilde{\omega}_{i,k}(t)\|^2 + 2\eta\delta_{i,k}(t)\Delta u_{i,k}(t)h^T\tilde{\omega}_{i,k}(t) \\ &\quad + \eta^2\delta_{i,k}^2(t)\|h\|^2\left(\Delta u_{i,k}(t)\right)^2.\end{aligned} \tag{19}$$

Since $\eta\delta_{i,k}(t)h \triangle u_{i,k}(t) \leq 0$, (19) follows from (17) and the proof is completed. ■

Lemma 2. (Boundedness of the estimation error) *The PPD estimation error satisfies*

$$|\delta_{i,k}(t)| \leq \varepsilon_{\max}|\Delta u_{i,k}(t)| + \kappa|\tilde{\omega}_{i,k}(t)|, \tag{20}$$

where $\kappa = h_{\max}\phi_{\max}$.

Proof. From the PPD estimation error $\delta_{i,k}(t)$, it follows that

$$\begin{aligned}\boldsymbol{\delta}_{i,k}(t) &= y_{i,k}(t+1) - y_{i,k}(t) - \hat{\phi}_{i,k}(t)\Delta u_{i,k}(t) \\ &= \Delta y_{i,k}(t+1) - \hat{\phi}_{i,k}(t)\Delta u_{i,k}(t) \\ &= \phi_{i,k}(t)\Delta u_{i,k}(t) - \hat{\phi}_{i,k}(t)\Delta u_{i,k}(t) \\ &= \left[\phi_{i,k}(t) - \hat{\phi}_{i,k}(t)\right]\Delta u_{i,k}(t).\end{aligned} \tag{21}$$

■

From Assumption 1, we have

$$\phi_{i,k}(t) = \omega_i^{*T} h(z_{i,k}(t)) + \varepsilon_{i,k}(t), \quad |\varepsilon_{i,k}(t)| \leq \varepsilon_{\max}, \tag{22}$$

where $\varepsilon_{i,k}(t)$ is the approximation error of the RBFNN. It then follows that

$$\phi_{i,k}(t) - \hat{\phi}_{i,k}(t) = \tilde{\omega}_{i,k}(t)h(z_{i,k}(t)) + \varepsilon_{i,k}(t). \tag{23}$$

Substituting into (21), we obtain

$$\delta_{i,k}(t) = \left[\tilde{\omega}_{i,k}(t)h(z_{i,k}(t)) + \varepsilon_{i,k}(t)\right]\Delta u_{i,k}(t). \tag{24}$$

Taking the absolute value of (24), it follows that

$$|\delta_{i,k}(t)| \leq \left[|\tilde{\omega}_{i,k}(t)h(z_{i,k}(t))| + |\varepsilon_{i,k}(t)|\right]|\Delta u_{i,k}(t)|. \tag{25}$$

From Assumption 2 and 3, we have

$$|\delta_{i,k}(t)| \leq \left(|\tilde{\omega}_{i,k}(t)|h_{\max} + \varepsilon_{\max}\right)|\Delta u_{i,k}(t)|. \tag{26}$$

Expanding, it follows that

$$|\delta_{i,k}(t)| \leq \varepsilon_{\max}|\Delta u_{i,k}(t)| + h_{\max}|\tilde{\omega}_{i,k}(t)||\Delta u_{i,k}(t)|. \tag{27}$$

According to Assumption 1, it is known that there exists $\phi_h(\max)$ such that $|\triangle u_{i,k}(t)| \leq c \cdot \phi_h(\max)$. A constant $\kappa = h_{\max}\phi_h(\max)$ is defined, and Lemma 2 is proven.

Theorem 1. *Under Assumptions 1–4, if the parameters satisfy*

$$0 < \eta < \frac{2}{\kappa^2\Delta u_{\max}^2} \quad , \quad \lambda > 0 \quad , \quad 0 < \rho < 2,$$

then

$$\lim_{k\to\infty}\sup_{t\in[0,t_{\min}]}\left|\xi_{i,k}^*(t)\right| = 0.$$

Proof. From the consistency error (3), it can be obtained that

$$\begin{aligned}\xi_{i,k}^*(t+1) &= \sum_{j\in N_i} a_{ij}\left(y_{j,k}^*(t+1) - y_{i,k}^*(t+1)\right) \\ &\quad + s_i\left(y_d(t+1) - y_{i,k}^*(t+1)\right).\end{aligned} \tag{28}$$

Substituting into (4), we obtain

$$\xi^*_{i,k}(t+1) = \xi^*_{i,k}(t) - d_i\phi_{i,k}(t)\Delta u_{i,k}(t) + \sum_{j\in N_i}\alpha_{ij}\phi_{i,k}(t)\Delta u_{i,k}(t) + s_i y_d(t+1), \tag{29}$$

where $d_i = \sum_{j\in N_i} a_{ij} + s_i$. From (15), we have

$$\xi^*_{i,k}(t+1) = \left[1 - \frac{\rho d_i^2\hat{\phi}^2_{i,k}(t)}{\lambda + d_i^2\hat{\phi}^2_{i,k}(t)}\right]\xi^*_{i,k}(t) + \zeta_{i,k}(t), \tag{30}$$

where $\zeta_{i,k}(t) = \sum_{j\in N_i}\alpha_{ij}\phi_{i,k}(t)\Delta u_{i,k}(t) + s_i y_d(t+1)$. ■

Let $\alpha_{i,k}(t) = 1 - \frac{\rho d_i^2\hat{\phi}^2_{i,k}(t)}{\lambda + d_i^2\hat{\phi}^2_{i,k}(t)}$. From Assumption 1 and the boundedness of $\phi_{i,k}(t)$, we have

$$\frac{d_i^2\phi^2_{\min}}{\lambda + d_i^2\phi^2_{\max}} \le \left|\frac{d_i^2\hat{\phi}^2_{i,k}(t)}{\lambda + d_i^2\hat{\phi}^2_{i,k}(t)}\right| \le \frac{d_i^2\phi^2_{\max}}{\lambda}. \tag{31}$$

Taking $\rho \in (0,2)$, it follows that

$$|\alpha_{i,k}(t)| = \left|1 - \rho\frac{d_i^2\hat{\phi}^2_{i,k}(t)}{\lambda + d_i^2\hat{\phi}^2_{i,k}(t)}\right| \le 1 - \Upsilon < 1, \tag{32}$$

where $\Upsilon = \min\left(\rho\frac{d_i^2\phi^2_{\min}}{\lambda + d_i^2\phi^2_{\max}}, 2 - \rho\frac{d_i^2\phi^2_{\max}}{\lambda}\right) > 0$.

The Lyapunov function on the time axis is taken as

$$V_t = \sum_{i=1}^{N}\left(\xi^*_{i,k}(t)\right)^2. \tag{33}$$

From (30) to (32), it follows that

$$\left|\xi^*_{i,k}(t+1)\right| \le (1-\Upsilon)\left|\xi^*_{i,k}(t)\right| + \left|\zeta_{i,k}(t)\right|. \tag{34}$$

Squaring both sides of (34), we have

$$\left(\xi^*_{i,k}(t+1)\right)^2 \le (1-\Upsilon)^2(\xi^*_{i,k}(t))^2 + 2(1-\Upsilon)\left|\xi^*_{i,k}(t)\right|\left|\zeta_{i,k}(t)\right| + \zeta^2_{i,k}(t). \tag{35}$$

Taking the sum of both sides of (35), it follows that

$$V_{t+1} \le (1-\Upsilon)^2 V_t + 2(1-\Upsilon) \times \sum_{i=1}^{N}\left|\xi^*_{i,k}(t)\right|\left|\zeta_{i,k}(t)\right| + \sum_{i=1}^{N}\zeta^2_{i,k}(t), \tag{36}$$

where $|\zeta_{i,k}(t)| \le \overline{a}\phi_{\max}\Delta u_{\max} + \overline{s}\Delta y_{d,\max} = \overline{\zeta}, \bar{a} = \max\sum_{j\in N_i} a_{ij}, \bar{s} = \max s_i$.

By the Cauchy–Schwarz inequality, we have

$$\sum_{i=1}^{N}\left|\xi^*_{i,k}(t)\right|\left|\zeta_{i,k}(t)\right| \le \sqrt{V_t}\sqrt{N}\overline{\zeta}. \tag{37}$$

Substituting into (36), we obtain

$$V_{t+1} \le (1-\Upsilon)^2 V_t + 2(1-\Upsilon)\sqrt{N}\sqrt{V_t}\overline{\zeta} + N\,\overline{\zeta}^2. \tag{38}$$

The Lyapunov function on the iteration axis is

$$V_k = \sum_{t=0}^{t_{\max}} V_t = \sum_{t=0}^{t_{\max}}\sum_{i=1}^{N}\left(\xi^*_{i,k}(t)\right)^2. \tag{39}$$

Taking the sum of (36) from $t=0$ to $t=t_{\max}$, it follows that

$$\sum_{t=0}^{t_{\max}} V_{t+1} \le (1-\Upsilon)^2\sum_{t=0}^{t_{\max}} V_t + 2(1-\Upsilon)\sum_{t=0}^{t_{\max}}\sum_{i=1}^{N}\left|\xi^*_{i,k}(t)\right|\left|\zeta_{i,k}(t)\right| + \sum_{t=0}^{t_{\max}}\sum_{i=1}^{N}\zeta^2_{i,k}(t). \tag{40}$$

From (37), we have

$$\sum_{t=0}^{t_{\max}}\sum_{i=1}^{N}\left|\xi^*_{i,k}(t)\right|\left|\zeta_{i,k}(t)\right| \le \sqrt{N}\overline{\zeta}\sum_{t=0}^{t_{\max}}\sqrt{V_t}. \tag{41}$$

Let $S_k = \sum_{t=0}^{t_{\max}} V_t$. By the Cauchy–Schwarz inequality, it follows that

$$\left(\sum_{t=0}^{t_{\max}}\sqrt{V_t}\right)^2 \le \left(\sum_{t=0}^{t_{\max}}1\right)\left(\sum_{t=0}^{t_{\max}}V_t\right) \le (t_{\max}+1)\,S_k, \tag{42}$$

thus

$$\sum_{t=0}^{t_{\max}}\sqrt{V_t} \le \sqrt{(t_{\max}+1)S_k}. \tag{43}$$

It can be obtained that

$$2(1-\Upsilon)\sum_{i=1}^{n}\left|\xi^*_{i,k}(t)\right|\left|\zeta_{i,k}(t)\right| \le 2(1-\Upsilon)\sqrt{N}\overline{\zeta}\sqrt{(t_{\max}+1)S_k}. \tag{44}$$

Similarly, we have

$$\sum_{t=0}^{t_{\max}}\sum_{i=1}^{N}\zeta^2_{i,k}(t) \le \sum_{t=0}^{t_{\max}} N\overline{\zeta}^2 = N\overline{\zeta}^2(t_{\max}+1). \tag{45}$$

By combining (44) and (45), (40) can be rewritten as

$$\sum_{t=0}^{t_{\max}} V_{t+1} \le (1-\Upsilon)^2\sum_{t=0}^{t_{\max}} V_t + 2(1-\Upsilon)\sqrt{N}\,\overline{\zeta}\sqrt{(t_{\max}+1)S_k} + N\overline{\zeta}^2(t_{\max}+1). \tag{46}$$

It further follows that

$$S_k \leq \frac{N\overline{\zeta}(t_{\max}+1)}{\Upsilon(1-\Upsilon)} + \delta_k, \tag{47}$$

where δ_k represents the disturbance term.

The Lyapunov function for the weight error update is constructed as

$$W_k = \sum_{i=1}^{N}\sum_{t=0}^{t_k} \|\omega_{i,k}(t)\|^2. \tag{48}$$

Considering adjacent iterations

$$\begin{aligned} W_{k+1} &= \sum_{i=1}^{N}\sum_{t=0}^{t_{k+1}} \|\tilde{\omega}_{i,k+1}(t)\|^2 \\ &= \sum_{i=1}^{N}\sum_{t=0}^{t_k} \|\tilde{\omega}_{i,k+1}(t)\|^2 \\ &\quad + \sum_{i=1}^{N}\sum_{t=t_k+1}^{t_{k+1}} \|\tilde{\omega}_{i,k+1}(t)\|^2, \end{aligned} \tag{49}$$

from (8), it can be obtained that

$$\sum_{i=1}^{N}\sum_{t=0}^{t_k} \|\tilde{\omega}_{i,k+1}(t)\|^2 = \sum_{i=1}^{N}\sum_{t=t_k}^{t_k} \|\tilde{\omega}_{i,k}(t)\|^2, \tag{50}$$

$$W_{k+1} \leq \mu W_k + \boldsymbol{\varepsilon}_k{}^{(w)}, \tag{51}$$

where $\mu < 1$,$\mathcal{E}_k$ is an infinitesimal quantity. It is recursively derived that

$$W_k \leq \mu_w^k W_0 + \sum_{j=0}^{k-1} \mu_w^j \varepsilon_{k-j}^{(w)}. \tag{52}$$

When $\mathcal{E}_k \to 0$, W_k converges.

The global Lyapunov function is constructed as

$$L_k = V_k + \frac{1}{\eta} W_k, \tag{53}$$

so

$$L_{k+1} = \mu L_k + \varepsilon_k, \tag{54}$$

where

$$\mu = \max\left(1 - \frac{\Upsilon}{2}, \mu_w\right) < 1,$$

$$\boldsymbol{\varepsilon}_k = c_1 \boldsymbol{\varepsilon}_{\max}^2 + c_2 \sum_{i=1}^{N} \|\boldsymbol{\omega}_i^* - \boldsymbol{\omega}_{i,k}(0)\|^2,$$

while c_1 and c_2 are constants. By Banach fixed-point theorem (also known as the contraction mapping principle), it follows that

$$L_k \leq \mu^k L_0 + \frac{\varepsilon}{1-\mu} \quad \left(\boldsymbol{\varepsilon} = \sup_k \boldsymbol{\varepsilon}_k\right) \tag{55}$$

when $k \to \infty, \lim\limits_{k\to\infty} L_k = 0 \Rightarrow \lim\limits_{k\to\infty} V_k = 0$, $\lim\limits_{k\to\infty} \sum\limits_{t=0}^{t_{\max}} \sum\limits_{i=1}^{N} (\xi_{i,k}^*(t))^2 = 0$.

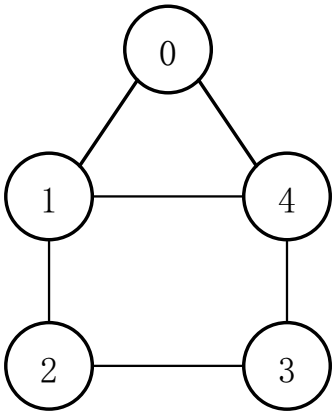


Fig. 1. System communication topology.

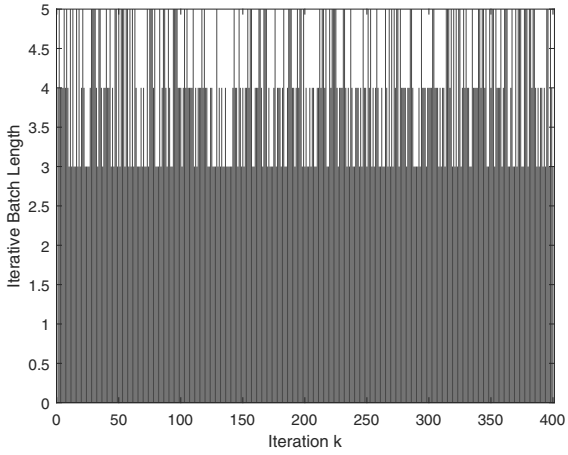


Fig. 2. Distribution of randomly varying iteration batches.

5. Simulation

Simulation studies are conducted in this section to validate the obtained results. A multi-agent system composed of four followers and one virtual leader is considered, with its communication topology illustrated in Fig. 1. The virtual leader is labeled as 0 and the followers are numbered 1–4. As observed from the communication topology, only followers 1 and 4 can directly receive information from virtual leader 0. Consequently, it can be concluded that

$$A = \begin{bmatrix} 0 & 1 & 0 & 1 \\ 1 & 0 & 1 & 0 \\ 0 & 1 & 0 & 1 \\ 1 & 0 & 1 & 0 \end{bmatrix},$$

$$D = \begin{bmatrix} 1 & 0 & 0 & 0 \\ 0 & 0 & 0 & 0 \\ 0 & 0 & 0 & 0 \\ 0 & 0 & 0 & 1 \end{bmatrix},$$

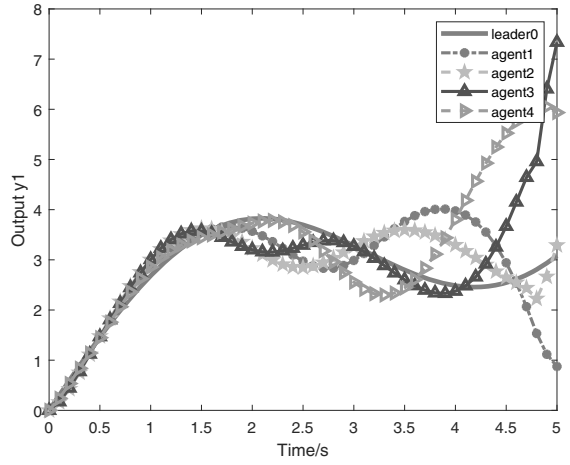


Fig. 3. Output component 1 of agents at the 50th iteration.

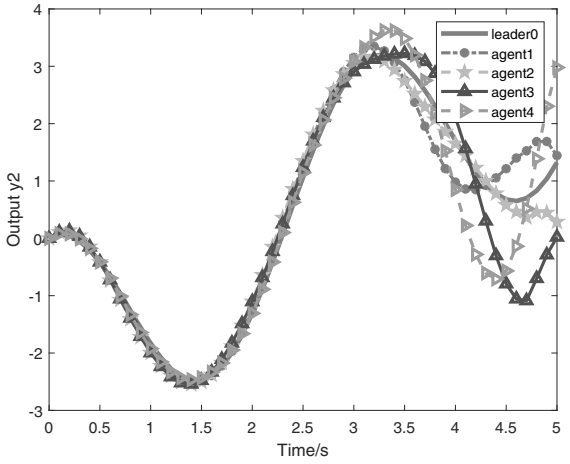


Fig. 4. Output component 2 of agents at the 50th iteration.

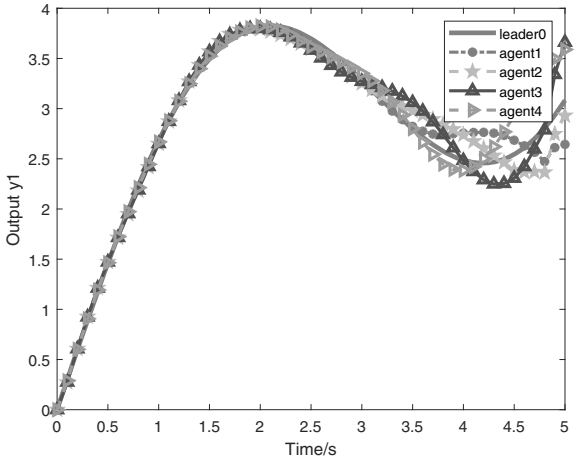


Fig. 5. Output component 1 of agents at the 150th iteration.

so

$$L = D - A = \begin{bmatrix} 1 & -1 & 0 & -1 \\ -1 & 0 & -1 & 0 \\ 0 & -1 & 0 & -1 \\ -1 & 0 & -1 & 1 \end{bmatrix}.$$

The systems are given as follows:

$$\begin{bmatrix} x_1(t+1) \\ x_2(t+1) \end{bmatrix} = \begin{bmatrix} \frac{1}{2}\cos x_1(t) + \frac{1}{5}x_2(t) \\ -\frac{1}{10}\sin x_2(t) \end{bmatrix} + \begin{bmatrix} 1 & 1.5 \\ 1 & -1 \end{bmatrix} \begin{bmatrix} u_1(t) \\ u_2(t) \end{bmatrix},$$

$$\begin{bmatrix} y_1(t) \\ y_2(t) \end{bmatrix} = \begin{bmatrix} 1 & 1 \\ 2 & -1 \end{bmatrix} \begin{bmatrix} x_1(t) \\ x_2(t) \end{bmatrix}.$$

Similarly to the findings of Xiong and Hou (2022), these coefficient matrices solely provide the input-output data of the system. Consider the desired trajectory of virtual leader 0 as

$$y_d(t) = \begin{bmatrix} t + 2\sin t \\ t + 2\cos 2t - 2 \end{bmatrix},$$

$t \in [0, 5]$,$t_s = 0.1$. For convenience of analysis, the initial states and the control inputs of all four agents are set as $x_0 = \begin{bmatrix} 0, 0 \end{bmatrix}^T$ and $u_0 = \begin{bmatrix} 0, 0 \end{bmatrix}^T$. The iteration batch length varies randomly between $T_{\min} = 3$ and $T_{\max} = 5$. Moreover, $\alpha = 0$,$r = 1$, $\eta = 0.5$, $\rho = 0.4$, $\lambda = 0.1$.

Figure 2 shows the distribution of randomly varying iteration batches with iteration counts. It can be observed that the iteration batch length exhibits randomness during each iteration.

Figures 3 and 4 show the comparisons between the two output components of the four agents and the desired trajectory at the 50th iteration, while Figs. 5 and 6 present the corresponding comparisons at the 150th iteration, and Figs. 7 and 8 display those at the 400th iteration. It can be observed that, as the number of iterations increases, the outputs of all four agents gradually approach the desired trajectory, achieving consensus control. Figures 9 and 10 illustrate the variations of the two input components of the four agents with respect to the iteration count. It can be observed that, as the number of iterations increases, the inputs of all four agents tend to converge toward consensus.

Figures 11 and 12 depict the variations of the two state components of the four agents with respect to the iteration count. It can be observed that, as the number of iterations increases, the states of all four agents tend to converge toward consensus.

Figures 13 and 14 show the variations of the two error components of the four agents with respect to the iteration count. It can be observed that, as the number of iterations increases, the errors of all four agents asymptotically approach zero, achieving stability.

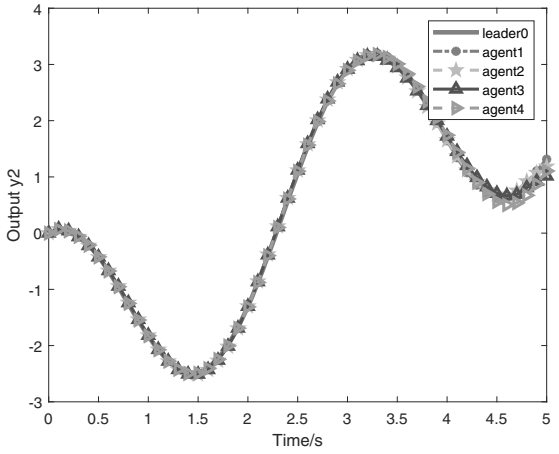


Fig. 6. Output component 2 of agents at the 150th iteration.

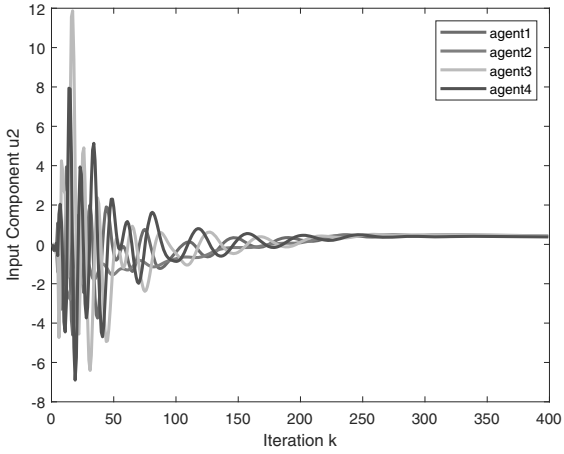


Fig. 9. Variation of the agent's input component 1.

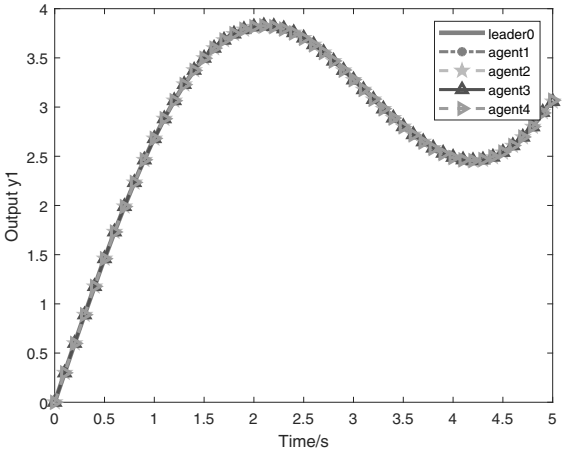


Fig. 7. Output component 2 of agents at the 400th iteration.

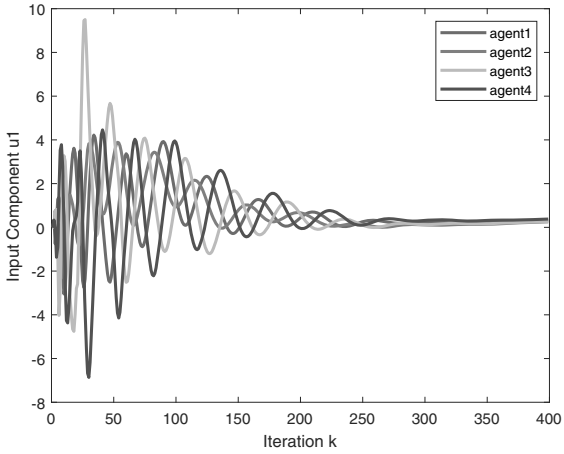


Fig. 10. Variation of the agent's input component 2.

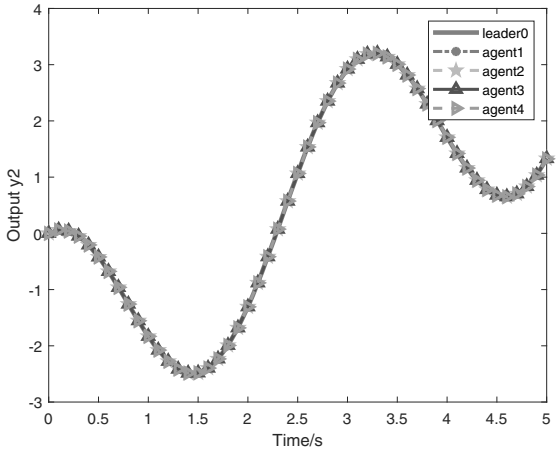


Fig. 8. Output component 2 of agents at the 400th iteration.

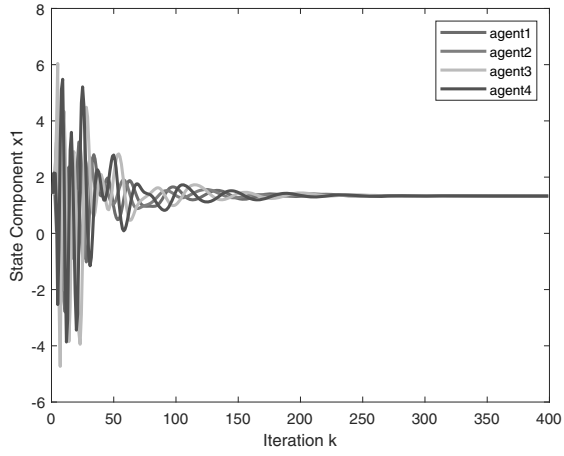


Fig. 11. Variation of the agent's state component 1.

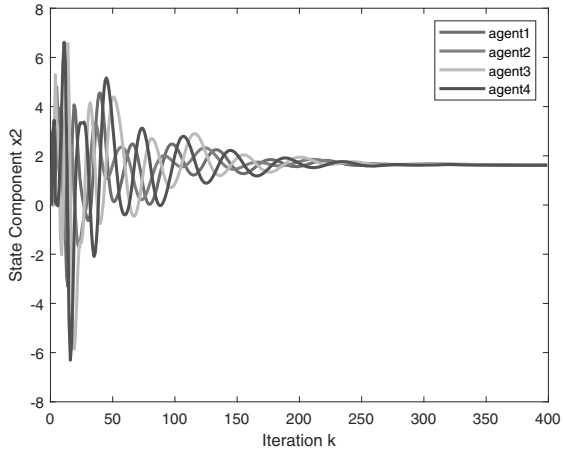


Fig. 12. Variation of the agent's state component 2.

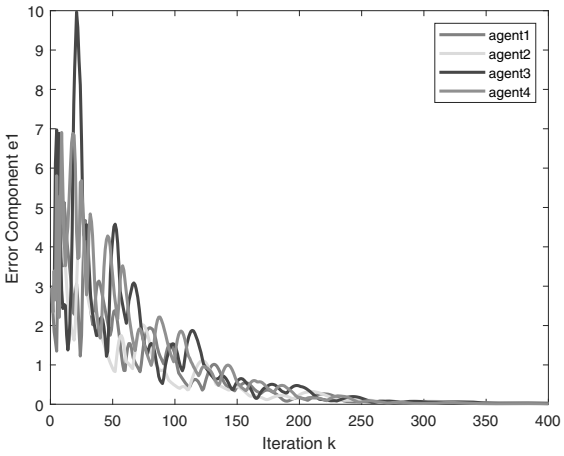


Fig. 13. Variation of the agent's error component 1.

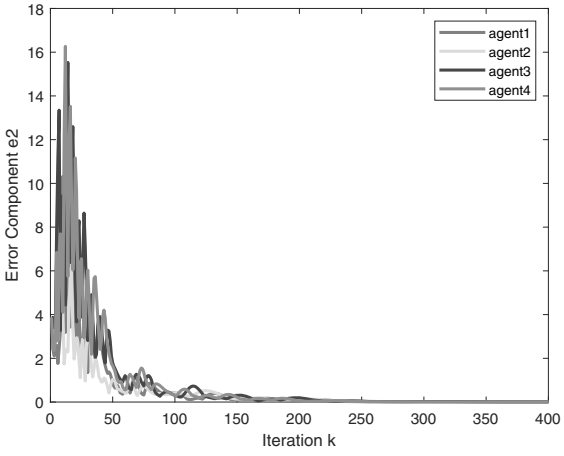


Fig. 14. Variation of the agent's error component 2.

6. Conclusion

Based on neural networks, this paper addressed the scenario where iteration batch lengths in multi-agent systems vary randomly with iteration counts. A fault model for missing iteration batches subject to random probability distributions was designed. Also, a novel data-driven adaptive iterative learning consensus control algorithm was proposed. The stability analysis of the system was rigorously conducted using Lyapunov functions, and sufficient conditions for consensus in multi-agent systems were derived through relevant mathematical deductions, ensuring that state consensus can still be achieved despite a missing iteration.

Acknowledgment

This work is supported by the National Natural Science Foundation of China under the grant no. 62103057. Also, the authors declare no conflict of interest.

References

Bu, X., Yu, Q., Hou, Z. and Qian, W. (2019). Model free adaptive iterative learning consensus tracking control for a class of nonlinear multiagent systems, *IEEE Transactions on Systems, Man, and Cybernetics: Systems* **49**(4): 677–686.

Dong, X., Zhou, Y., Ren, Z. and Zhong, Y. (2016). Time-varying formation control for unmanned aerial vehicles with switching interaction topologies, *Control Engineering Practice* **46**: 26–36.

Fu, J., Wen, G., Yu, W. and Ding, Z. (2017). Finite-time consensus for second-order multi-agent systems with input saturation, *IEEE Transactions on Circuits and Systems II: Express Briefs* **65**(11): 1758–1762.

Gao, H., Cheng, B., Wang, J., Li, K., Zhao, J. and Li, D. (2018). Object classification using CNN-based fusion of vision and LiDAR in autonomous vehicle environment, *Control Theory & Applications* **35**(10): 1415–1421.

Hou, Z., Chi, R. and Gao, H. (2017). An overview of dynamic-linearization-based data-driven control and applications, *IEEE Transactions on Industrial Electronics* **64**(5): 4076–4090.

Jiaqi, L., Xuhui, B. and Jian, L. (2018). Iterative learning consensus tracking control for a class of multi-agent systems with data dropouts, *Computer Engineering and Applications* **54**(20): 42–47.

Jinli, G., Xuhui, B. and Lizhi, C. (2023). Model free adaptive iterative learning tracking control for multi-agent systems under DOS attacks, *Control Theory & Applications* **40**(6): 977–985.

Li, D. and Gao, H. (2018). A hardware platform framework for an intelligent vehicle based on a driving brain, *Engineering* **4**(4): 464–470.

Li, X., Xu, J.-X. and Huang, D. (2014). An iterative learning control approach for linear systems with randomly varying trial lengths, *IEEE Transactions on Automatic Control* **59**(7): 1954–1960.

Liang, J.-Q., Bu, X.-H., Wang, Q.-F. and He, H. (2019). Iterative learning consensus tracking control for nonlinear multi-agent systems with randomly varying iteration lengths, *IEEE Access* **7**: 158612–158622.

Liu, T. and Hou, Z. (2023). Model-free adaptive iterative learning containment control for unknown heterogeneous nonlinear mass with disturbances, *Neurocomputing* **515**: 121–132.

López-Estrada, F.-R., Darias, H., Puig, V., Valencia-Palomo, G., Domínguez-Zenteno, J. and Guerrero-Sánchez, M.-E. (2024). Cooperative convex control of multiagent systems applied to differential drive robots, *International Journal of Applied Mathematics and Computer Science* **34**(2): 199–210, DOI: 10.61822/amcs-2024-0014.

Lv, Y., Zhang, H., Wang, Z. and Yan, H. (2024). Distributed localization for multi-agent systems with random noise based on iterative learning, *IEEE Transactions on Neural Networks and Learning Systems* **35**(1): 952–960.

Peng, H., Lin, N. and Chi, R. (2024). Gain-varying P-type ILC for nonlinear multi-agent systems against FDI attacks, *2024 IEEE 13th Data Driven Control and Learning Systems Conference (DDCLS), Kaifeng, China*, pp. 972–976.

Postoyan, R., Bragagnolo, M.C., Galbrun, E., Daafouz, J., Nešić, D. and Castelan, E.B. (2015). Event-triggered tracking control of unicycle mobile robots, *Automatica* **52**: 302–308.

Rehan, M., Jameel, A. and Ahn, C.K. (2018). Distributed consensus control of one-sided Lipschitz nonlinear multiagent systems, *IEEE Transactions on Systems, Man, and Cybernetics: Systems* **48**(8): 1297–1308.

Shen, D., Zhang, W. and Xu, J.-X. (2016). Iterative learning control for discrete nonlinear systems with randomly iteration varying lengths, *Systems & Control Letters* **96**: 81–87.

Wang, C., Wang, X. and Ji, H. (2016). Leader-following consensus for a class of second-order nonlinear multi-agent systems, *Systems & Control Letters* **89**: 61–65.

Wu, J., Dai, X., Tian, S. and Huang, Q. (2023). Iterative learning consensus control of nonlinear impulsive distributed parameter multi-agent systems, *European Journal of Control* **71**: 100785.

Xiao, G., Wang, J. and Meng, D. (2023). Adaptive finite-time consensus for stochastic multiagent systems with uncertain actuator faults, *IEEE Transactions on Control of Network Systems* **10**(4): 1899–1912.

Xie, G., Gao, H., Qian, L., Huang, B., Li, K. and Wang, J. (2018). Vehicle trajectory prediction by integrating physics- and maneuver-based approaches using interactive multiple models, *IEEE Transactions on Industrial Electronics* **65**(7): 5999–6008.

Xiong, S. and Hou, Z. (2022). Data-driven formation control for unknown MIMO nonlinear discrete-time multi-agent systems with sensor fault, *IEEE Transactions on Neural Networks and Learning Systems* **33**(12): 7728–7742.

Zhang, T. and Li, J. (2024). Quantized iterative learning control for nonlinear multi-agent systems with limited information communication and input saturation, *Journal of the Franklin Institute* **361**(3): 1620–1630.

Zhang, T., Li, N. and Chen, J. (2024a). Quantized iterative learning control for nonlinear multi-agent systems with initial state error, *Systems & Control Letters* **186**: 105756.

Zhang, Z., Ma, T., Su, X. and Ma, X. (2024b). Impulsive consensus of one-sided Lipschitz multi-agent systems with deception attacks and stochastic perturbation, *IEEE Transactions on Artificial Intelligence* **5**(3): 1328–1338.



Xingjian Fu received his PhD at the School of Automation, University of Science and Technology Beijing, China, in 2005. Currently, he is a professor in Beijing Information Science and Technology University. He has published about 100 papers. He is a committee member of the Mechanical Industry Automation Branch of the China Mechanical Engineering Society, as well as a member of the China Automation Society and the Chinese Association for Artificial Intelligence. His research interests include intelligent control, robust fault-tolerant control and moving body control.



Yuhan Li received his BS degree in engineering from the Nantong Institute of Technology in 2022, and is currently pursuing an MS degree at the School of Automation, Beijing Information Science and Technology University. His research interests include iterative learning control strategies for multi-agent systems and data-driven control.

Received: 12 October 2025
Revised: 26 May 2026
Accepted: 2 June 2026